

Effects of Mechanical Activation Time and Speed on the Steel Slag Powder Characteristics for Wastewater Treatment

Zainudin Muhammad Aiman¹, Aziz Muhamad Afif¹, Yusoff Mahani^{1,*}, Teo Pao Ter¹, Razali Mohd Hasmizam²

¹Faculty of Bioengineering and Technology, Universiti Malaysia Kelantan, 17600 Jeli, Kelantan, Malaysia

²Faculty of Science and Marine Environment, Universiti Malaysia Terengganu, 21030 Kuala Nerus, Terengganu, Malaysia

*Corresponding author: mahani@umk.edu.my

ARTICLE INFO

Received: 5 April 2024
Accepted: 15 May 2024
Online: 27 June 2024
eISSN: 3036-017X

ABSTRACT

Steel slag has a high iron content, which could be advantageous in producing iron-rich salt sources for wastewater treatment. Producing iron-rich residue from steel slag to be applied as ferrous sulfate demanded powder activation to achieve high absorption efficiency during coagulation. Mechanical activation via high-energy ball milling was one of the methods that could minimize the poor grindability of steel slag. The effect of milling time (2 h, 8 h, 10 h, and 20 h) and milling speed (200 rpm, 250 rpm, and 300 rpm) on the powder characteristics were observed on the as-milled powder. The phase identification of mineral composition presented the gehlenite, larnite, magnetite, quartz low, kyanite, and wuestite similar to that in raw steel slag. These phases' crystallinity was more pronounced at 20 h and 300 rpm, indicating that the internal structure of the powder was altered through mechanical deformation during the milling process. The morphology of the as-milled steel slag with increasing milling time and speed showed a reduction of particle size and was more uniform. Milling time (up to 20 h) and speed (300 rpm) were identified as optimum parameters for producing the finest particle size, which is also supported by its surface area (3.356 m²/g). This study has obtained that increasing milling parameters in high-energy ball milling and speed could reduce the particle size of steel slag powder. The powder might be applied as a reducing agent in wastewater treatment.

Keywords: Steel slag; High-energy milling; Wastewater treatment; Reducing agent

1. Introduction

Treating wastewater is an essential process to protect the environment and human health. Different treatment technologies have been developed to remove pollutants and contaminants from wastewater, including heavy metals. The use of wastewater treatment is an innovative approach that has gained attention in recent years, which not only helps treat wastewater but also aids in managing waste effectively. They also offer several benefits, including cost-effectiveness, waste reduction, and environmental sustainability. However, there are also challenges associated with this approach, such as the need for pre-treatment of waste, the potential release of contaminants from the waste into the treated water, and proper disposal after its use in wastewater treatment.

One alternative for wastewater treatment is the utilization of recycled steel slag. Steel slag is an essential by-product produced when purifying molten steel. Huge steel slag waste is generated from the electric arc furnace, blast furnace, ladle furnace, and basic oxygen furnace process. The composition of steel slag waste is a mixture of ferrous oxide (FeO), iron oxide (Fe₂O₃), silicon dioxide (SiO₂), calcium oxide (CaO), alumina (Al₂O₃), and magnesium (II) oxide (MgO) [1]. This by-product is often disposed of through landfilling, which causes pollution in the surrounding area. Several efforts have been made to recycle steel slag into more useful industrial products such as building materials, fertilizer, and chemical processes [2]. Steel slag contains a high iron content; therefore, there is a lot of effort to utilize its iron-rich content. For example, recycled iron is used in the ironmaking and steelmaking processes by limiting high-cost steel scrap and iron ores [3]. Also, because high iron oxide has been found in steel slag, it could be utilized as a fluxing agent for conventional ceramic products [4]. Steel slag could treat wastewater due to its high iron content. Their utilization predominantly focuses on their ability to effectively and efficiently absorb heavy metal ions and organic pollutants [5]. Steel slag effectively removes copper and lead from wastewater through adsorption, precipitation, and ion exchange mechanisms [6]. In addition, steel slag was also found useful as a coagulant in the form of ferrous sulfate, which effectively reduces turbidity and removes suspended solids from wastewater [7].

To effectively treat wastewater, it is necessary to finely grind steel slag to reduce its particle size and optimize oxidation reactions. Small particle size may help to improve reactivity and better flocculation. Optimizing the oxidation reaction is crucial for improving heavy metal removal by introducing various oxide components that form insoluble compounds, which can be easily eliminated. High-energy ball milling techniques have been a reliable method for producing metal powder, which could be one of the suitable methods for making a refined structure of steel slag before it proceeds to the sintering or magnetic separation process for iron recovery. However, the properties of poor grindability of steel slag waste have become a challenge in producing fine particle sizes of iron powder [8]. The most influential milling parameters are milling time and milling speed. Thus, this study will optimize milling time and speed using a high-energy ball mill to produce iron powder from steel slag. This research aims to study the optimum milling time and speed for producing iron powder from steel slag using high-energy ball milling.

2. Materials and Methods

The steel slag was obtained from the local steelmaking industry. The milling process was performed using a planetary ball mill (DECO-PBM-V-0.4L) for 2, 4, 8, and 10 h with milling speeds of 200, 250, and 300 rpm. The milling time and speed were chosen carefully to prevent severe agglomeration that could occur because steel slag consists of various compositions. The ball and jar used are made of zirconia. The ball size was fixed at 10 mm diameter while the ball-to-powder ratio (BPR) was at 10:1. X-ray diffraction (XRD) Bruker D2 Phaser was used to determine the phase identification of the as-received and the as-milled steel slag. The step size was fixed at 0.02° with 2θ angle from 10° to 90°. The elemental composition of as-received steel slag was determined by portable X-ray fluorescence (XRF, Bruker S1 Titan 800). Scanning electron microscope (SEM) JEOL-JSM IT-100 with back-scattered electrons (BSE) was used to study the morphology of the as-milled steel slag powder. The Brunauer–Emmett–Teller equation (BET) was used to determine the surface area of the as-milled powder and was analyzed using Micromeritics ASAP 2020 V3.04H (Micromeritics®). All samples were degassed at 300°C for 6 h before analysis.

3. Results and Discussion

Fig. 1 shows the XRD pattern of as-received steel slag powder. The peak pattern was analyzed and identified as andradite, gehlenite, larnite, magnetite, quartz low, kyanite, and wuestite. The XRF result also confirmed these compounds, as shown in Table 1. The primary chemical components of as-received steel slag are CaO, SiO₂, Fe₂O₃, Al₂O₃, MgO, MnO, and Fe. The oxide-based phases such as MgO, FeO, MnO, and CaO present in steel slag powder made it challenging to mill into fine size, resulting from the intrinsic material properties of these metal oxides [9]. For instance, MgO possesses a high hardness and inter-particle solid bonding, resulting in significant resistance to fracture during milling. The interaction of these oxides makes up the chemical and physical properties of steel slag and plays an essential role in determining milling behavior. In addition, steel slag also demonstrates noteworthy variability, influenced by a combination of factors, including the steel type, raw materials, and the smelting process.

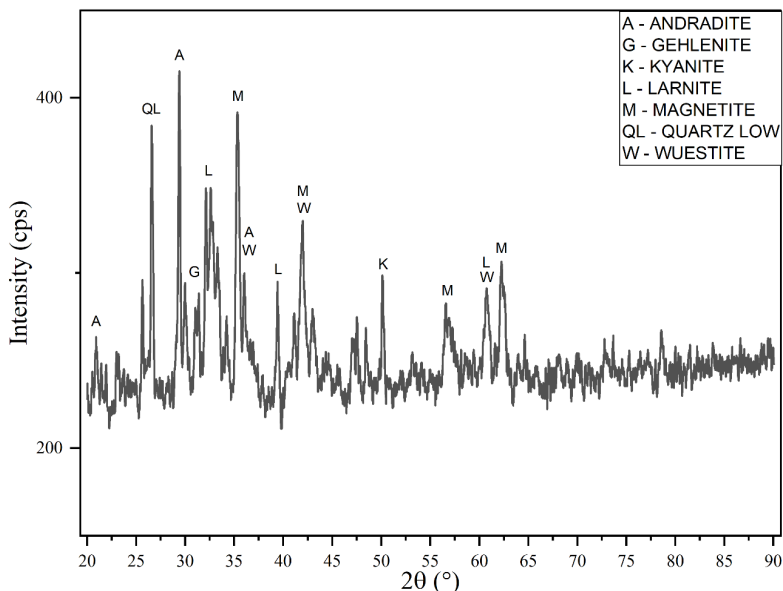


Fig. 1. XRD patterns of as-received steel slag powder

Table 1. XRF analysis of as-received steel slag powder

Element/compound	%	Element/compound	%
MgO	3.172	Zn	0.229
Al ₂ O ₃	5.432	Ga	0.002
SiO ₂	18.166	As	0.003
P	0.336	Sr	0.034
S	0.076	Y	0.001
K ₂ O	0.112	Zr	0.010
Ca	16.471	Ag	0.003
Ti	0.254	Sn	0.018
V	0.126	Ba	0.177
Cr	0.349	Ce	0.028
Mn	2.279	Pb	0.009
Fe	12.217		

The XRD patterns of the as-milled steel slag powder at different milling times (2, 8, 10 and 20 h) for milling speeds of 200, 250, and 300 rpm are shown in Fig. 2. The peaks identified were andradite, gehlenite, larnite, magnetite, quartz low, kyanite, and wuestite that were typically observed in steel slag which having high magnetite (10 to 35%) [10] and quartz (5 to 15%) contents [11]. More pronounced peaks of these phases were observed from 2 h to 20 h. The most substantial peak at $2\theta = 26^\circ$ for quartz low was widened when milling time increased to 10 h until 20 h for 250 rpm and 300 rpm. The peak broadening indicates that the crystallite dimension changes at the crystallographic plane. This study also found that milling speed had a more significant impact than milling time on the internal structure of steel slag powder after 20 h of milling. 250 to 300 rpm changes the structure of low quartz compared to the other stages because quartz is made of Si-O bonds easily broken by external deformation [12].

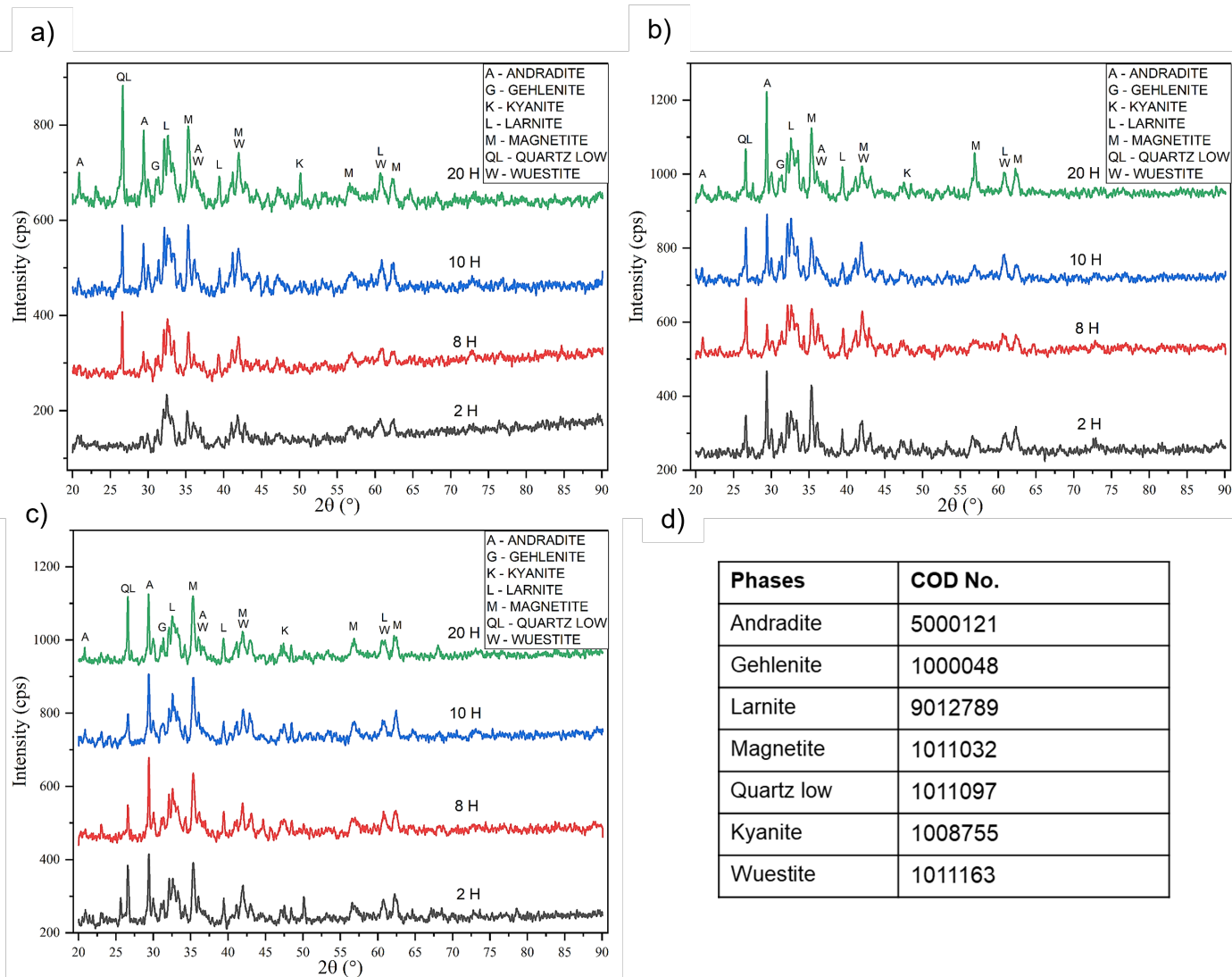


Fig. 2. XRD patterns of as-milled steel slag powder at different milling times for milling speeds of a) 200 rpm, b) 250 rpm, c) 300 rpm, d) COD number of the phases

The SEM images of the as-milled steel slag powder observed the particle size at different milling speeds (200 rpm, 250 rpm, and 300 rpm) and milling time (10 h and 20 h) is shown in Fig. 3. The particle of steel slag was distributed in an irregular shape and large particle sizes from 200 to 300 rpm at 20 h of milling. Increasing milling speed, the powder particle could decrease in size, and a finer structure would be produced [13]. Moreover, the effect of milling time was significant, evidenced by the distribution of particles from milled 10 h and 20 h. 10 h was insufficient to produce finer powder even at 300 rpm milling speed. The collision due to centrifugal force in high-energy ball milling would crush steel slag powder at 300 rpm milling speed. However, it must also be prolonged up to 20 h to produce the finest particle size. Therefore, by increasing milling time, the particle size of slag powder was reduced since that was enough energy impact to crush the steel slag in smaller sizes during the milling process in high-energy ball milling. It was observed that the chemical composition of the slag influences the shape and size of steel slag particles [14], as indicated in the XRD results (Figs. 1 and 2).

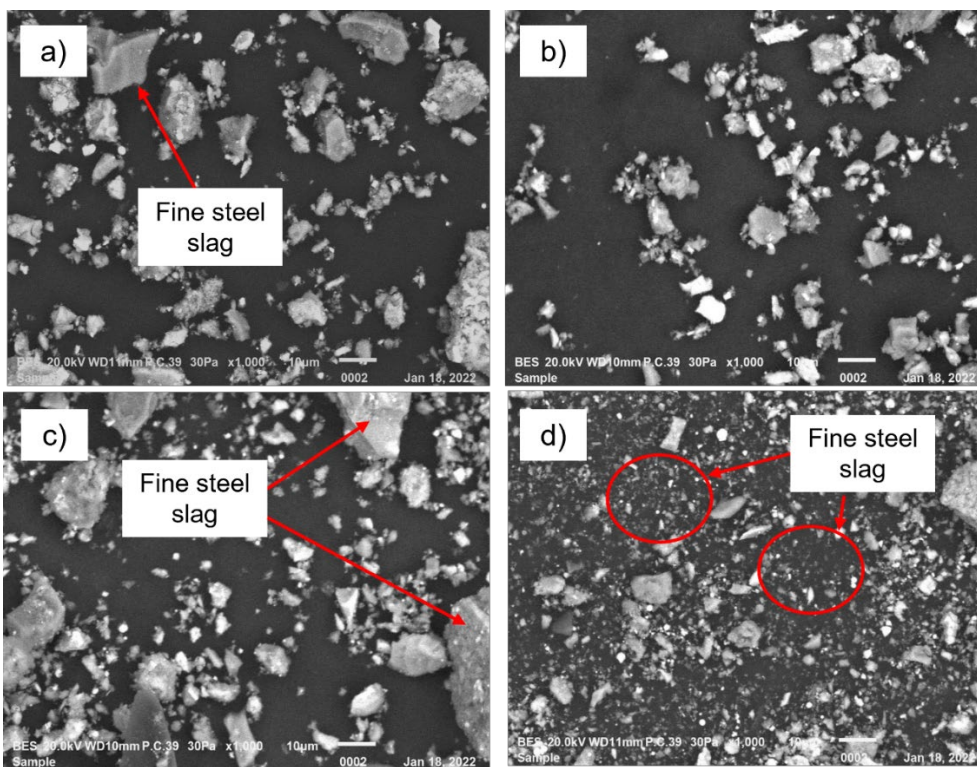


Fig. 3. SEM images of as-milled steel slag powder milled at a) 20 h milling time and 200 rpm, b) 20 h milling time and 250 rpm, c) 10 h milling time and 300 rpm, d) 20 h milling time and 300 rpm for 1000x magnifications

Table 2 shows the Brunauer Emmett Teller (BET) surface area, total pore volume, and pore width of the as-milled steel slag powder at milling speeds of 200 rpm, 250 rpm, and 300 rpm for milling times of 2 h and 20 h. An increase in milling speed reduces powder particle size, represented by a SEM image, and contributes to a lower surface area [15]. However, the surface area of the as-milled steel slag is reduced with increasing milling time (until 20 h) due to the agglomeration of fine particles. The low surface area at 20 h of milling was similar to a study by Yang et al. [16]. The larger pores of 60 – 70 nm contribute most to the pore volume of the steel slag for all milling time and speed. Adsorption efficiency is reduced when the pore size (pore width) is too large, and the surface area is too small. If the pore width is excessively large, the adsorbate molecules may become less to interact effectively with the adsorbent surface, thereby reduce the adsorption efficiency.

Table 2. BET surface area, total pore volume, and pore width of milled steel slag powder at different milling speeds and milling time

Milling time (h)	Milling speed (rpm)								
	300	250	200	300	250	200	300	250	200
	Surface area (m ² /g)			Total pore volume (cm ³ /g)			Pore width (nm)		
2	3.008	3.356	0.938	0.020	0.020	0.004	68.257	61.862	59.478
20	2.829	2.846	2.772	0.019	0.022	0.018	70.796	76.718	64.888

4. Conclusion

The effect of various milling parameters on the production of steel slag powder through high-energy ball milling was investigated. The study examined phase identification, morphology, and surface area. The results indicate that particle size reduction was influenced by milling time and speed, while the phase composition of the steel slag was less significantly affected. Milling speed was found to have a more significant influence on the broadening of the peaks than milling time. The as-milled steel slag has suitable characteristics for wastewater treatment applications, as its surface area is comparable to that of the properties of large pores. The optimal condition of the milling parameters to obtain fine particle steel slag was 20 h with 300 rpm, resulting in a surface area of 3.356 m²/g.

Acknowledgements

The authors would like to thank Universiti Malaysia Kelantan (UMK) for the equipment and the Malaysia Ministry of Higher Education's financial support for the Fundamental Research Grant (FRGS/1/2020/TK0/UMK/02/10).

References

- [1] Dhoble YN, Ahmed S. Sustainability of wastewater treatment in subtropical region: aerobic vs anaerobic process, *J Mater Cycles Waste Manag*, 2018;20:1373-82.
- [2] Gao D, Wang FP, Wang YT, Zeng YN. Sustainable utilization of steel slag from traditional industry and agriculture to catalysis, *Sustain*, 2020;12:9295.
- [3] Ma N, Houser J, Wood L, Lewis R, Hill DE, Maximizing the values of steelmaking slags, *J Sustain Metall*, 2017.
- [4] Teo PT, Anasyida AS, Kho CM, Nurulakmal MS. Recycling of Malaysia's EAF steel slag waste as novel fluxing agent in green ceramic tile production: Sintering mechanism and leaching assessment, *J Clean Prod*, 2019;241:118144.
- [5] Solanki C. Utilization of Steel Slag for Wastewater Treatment: A Review. In: Kondraivendhan B, Modhera CD, Matsagar V, editors. *Sustainable Building Materials and Construction*. Singapore: Springer Nature Singapore; 2022. p. 409-14.
- [6] Wang L, Fu P, Ma Y, Zhang X, Zhang Y, Yang X, Steel slag as a cost-effective adsorbent for synergic removal of collectors, Cu(II) and Pb(II) ions from flotation wastewaters, *Miner Eng*, 2022;183:107593
- [7] Abdel-Basser LT, Mohamed EA, Omran KA, Ismail MM, Mohamed FM, Switching of iron coagulants from steel residue for wastewater treatment, *Desalin. Water Treat*, 2024;319:100473.
- [8] Li M, Lu Y, Liu Y, Chu J, Zhang T, Wang W. Influence of the steel slag particle size on the mechanical properties and microstructure of concrete. *Sustain*, 2024; 16(5):2083
- [9] Martins ACP, Franco de Carvalho JM, Costa LCB, Andrade HD, de Melo TV, Ribeiro JCL, Pedroti LG, Peixoto RAF, Steel slags in cement-based composites: An ultimate review on characterization, applications and performance, *Constr Build Mater*, 2021;291:123265.
- [10] Jiang L, Bao Y, Chen Y, Liu G, Zhang X, Han F, Yang Q, Structural characteristics and hydration kinetics of oxidized steel slag in a CaO-FeO-SiO₂-MgO system. *High Temp Mater Process*, 2019;38:290-300.
- [11] Mombelli D, Mapelli C, Barella S, Gruttadauria A, Le Saout G, Garcia-Diaz E. *J Hazard Mater*, 2014;279:586-96.
- [12] Tiecher F, Florindo RN, Vieira GL, Gomes MEB, Dal Molin DCC, Lermen RT. Influence of the quartz deformation structures for the occurrence of the alkali-silica reaction, *Mater (Basel)*. 2018;11.
- [13] Bouaziz A, Hamzaoui R, Guessasma S, Lakhel R, Achoura D, Leklou N. Efficiency of high energy over conventional milling of granulated blast furnace slag powder to improve mechanical performance of slag cement paste. *Powder Technol*, 2016;308:37-46.
- [14] Li W, Xue X. Effect of the cooling regime on phase transformation and chromium enrichment in stainless steel slag. *Ironmaking Steelmaking*. 2018;46:1-7.
- [15] Cikmit AA, Tsuchida T, Kang G, Hashimoto R, Honda H. *Soil Found*, 2019;59:1385-98.
- [16] Yang L, Qian X, Wang Z, Li Y, Bai H, Li H. *Ad Sci Technol*, 2018; 36:1160-77.